EVALUATION OF THE WAKE OF AN AGRICULTURAL GROUND SPRAYER WITH THE WIND FROM ANY DIRECTION

M. E. Teske, H. W. Thistle, R. L. Petersen, T. C. R. Lawton, S. A. Guerra, T. G. Funseth

ABSTRACT. *Additional wind tunnel measurements of wind direction effects on the wake of a subscale tractor, tank, and spray boom model (representing a typical ground sprayer and henceforth referred to as a "spray rig") are presented to demonstrate the behavior of the dominant air motions responding to the presence of a spray rig. The approach measures the velocity and turbulence levels (in three directions) with the wind blowing from five angles (from directly toward the front of the tractor to directly toward the back of the tractor in 45° increments). The results quantify the effect on wind direction and turbulence level by the presence of the spray rig model. The goal of this effort is to combine and analyze these measurements to describe the full-scale wake of a specific tractor/tank/spray boom combination. In this way, the wake model will augment local atmospheric and surface effects to better predict the behavior of material released from nozzles on a spray boom during actual ground sprayer operation.*

Keywords. *AGDISP, Ground sprayer, Subscale model, Tractor wake, Wind tunnel.*

A recent article (Teske et al., 2015) detailed the velocity and turbulence effects around a subscale tractor, tank, and spray boom in a wind tunnel due to head winds (0°) toward the front of the tractor. This work was undertaken in an effort to provide a picture of the fluid dynamics around a typical ground sprayer as a possible aid in developing an applied mechanistic ground sprayer model and its model validation. Such a model was suggested by Teske et al. (2009) based on the same modeling approach used in AGDISP (Teske et al., 2003) for aerial spraying. Currently, AGDISP does not have a tractor wake model, only a description of the wind speed and direction toward the spray boom and the initial droplet speed from the nozzles. This article extends the flow field description around the tractor/boom combination to include the effects of wind direction at 45°, 90° (side wind), 135°, and 180° (tail wind).

As a step toward describing the details of the wake behind a tractor/tank/spray boom combination (a "spray rig"), the USDA Forest Service conducted two subscale model tests that simulated the wake effects around a generic John Deere tractor. The goal of these efforts was to present a more detailed look at the wake generated by a specific spray rig, in the expectation of describing the full-scale velocity and turbulence fields for modeling purposes. This article summarizes the wind tunnel results and parameterizes the velocity and turbulent energy fields.

The wake of a spray rig is complex, with the wake responding to ambient wind effects, the tractor body, boom geometry, sprayer sheet blockage from the nozzle effluent, tractor thermal exhaust and engine heating, tire motion, and surface effects from the ground and crop. It seems instructive to grasp what details can be obtained from simplified studies before attempting full-scale field experiments or undertaking extensive computational fluid dynamics simulations. Such an approach is therefore well suited for wind tunnel examination.

APPROACH

The wind tunnel used for wake mapping is a closed-circuit boundary-layer wind tunnel with a 20.7 m long and 3.66 m wide test section, described previously by Teske et al. (2015). An accurate 1:25 scale model of a typical spray rig was mounted on a turntable so that the wind could approach the scale model from any direction. Figure 1 is a picture of the wind tunnel, looking upwind, with the scale model positioned at 45° to the flow direction. Figure 2 illustrates the five wind directions explored in the tests. The absolute right-handed coordinate system has X pointing down the tunnel, Y pointing perpendicular to the left of X, and Z pointing upward. A reference right-handed coordinate system for each wind direction has x pointing in the direction of the wind, y pointing perpendicular to the left of x, and z pointing upward. Table 1 summarizes the locations of the measurement planes normal to the wind direction, referenced to the center of the spray boom.

Submitted for review in March 2016 as manuscript number MS 11844; approved for publication by the Machinery Systems Community of ASABE in July 2016.

Mention of company or trade names is for description only and does not imply endorsement by the USDA. The USDA is an equal opportunity provider and employer.

The authors are **Milton E. Teske, ASABE Member,** Senior Associate, Continuum Dynamics, Inc., Ewing, New Jersey; **Harold W. Thistle, ASABE Member,** Program Manager, USDA Forest Service, Morgantown, West Virginia; **Ronald L. Petersen,** Vice-President, **Tom C. R. Lawton,** Systems Engineering Manager, and **Sergio A. Guerra,** Senior Environmental Engineer, CPP, Inc., Fort Collins, Colorado; **Travis G. Funseth, ASABE Member,** Senior Design Engineer, John Deere Des Moines Works, Des Moines, Iowa. **Corresponding author:** Milton Teske, Continuum Dynamics, Inc., 34 Lexington Ave., Ewing, NJ 08616; phone: 609-538-0444; milt@continuum-dynamics.com.

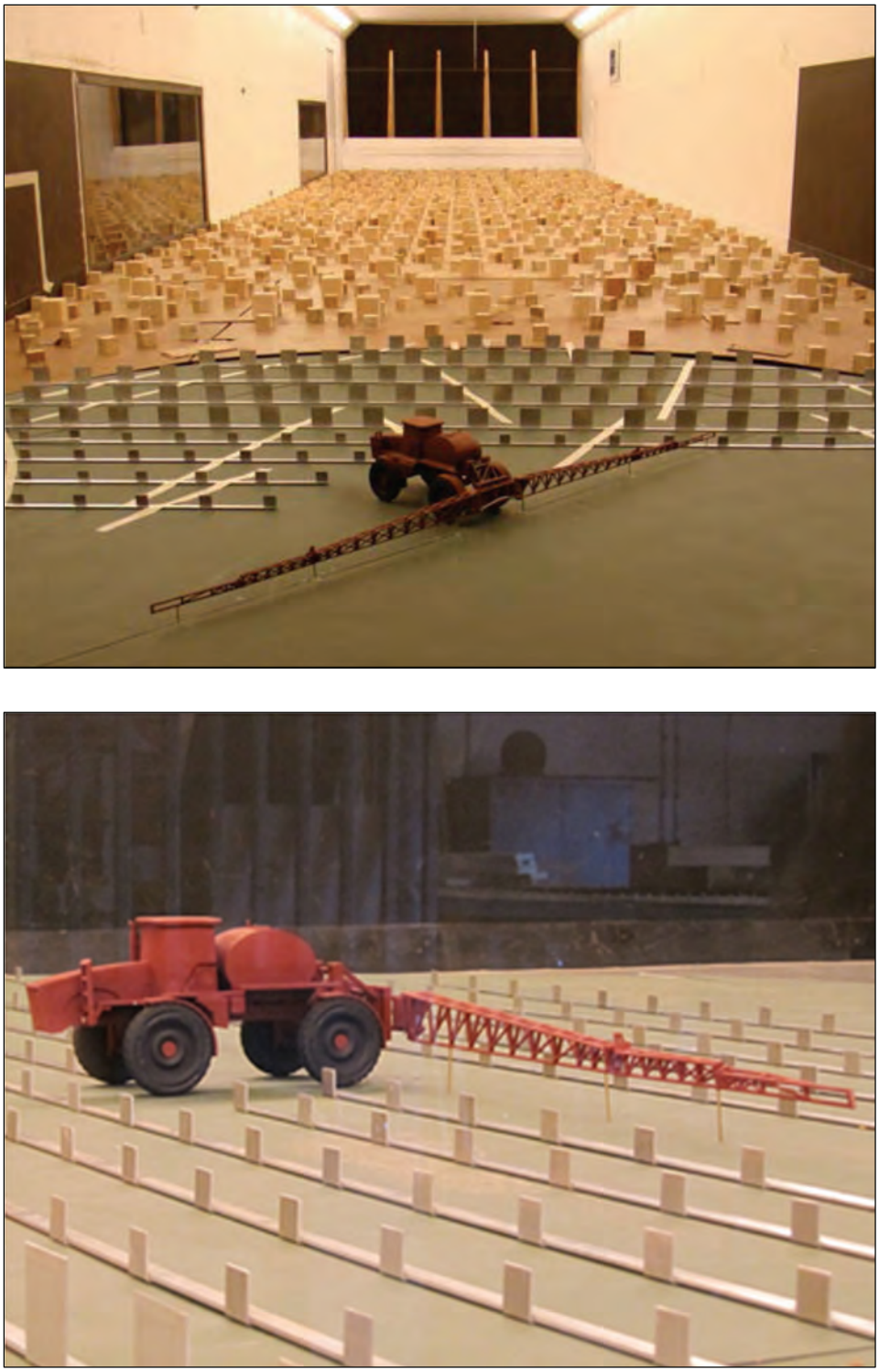

Figure 1. (top) Layout of the tunnel looking upwind with the spray rig rotated 45° to the wind and (bottom) side view of the scale model at 0° to the wind. The locations of the roughness elements are adjusted depending on wind direction and the desired probe measurement locations.

The wind tunnel included a computer-controlled traverse system that could map velocity (and other flow properties) at any *x*-*y*-*z* location to a high degree of accuracy (±5 mm in the *X* direction, ±1 mm in the *Y* direction, and ±0.5 mm in the *Z* direction). A boundary layer profile generation system, comprising a trip, spires, and a development fetch of around 15.2 m of 5 cm and 10 cm cuboid roughness elements, was placed upstream of the model (roughness elements were spaced more uniformly near the model, so as to facilitate wake measurements there). The roughness elements generated surface roughness suggestive of 10 to 18 cm high grass (Hansen, 1993). Measurements were made with an Aeroprobe 5-port probe (Aeroprobe Corp., Christiansburg, Va.), a compact 3.175 mm diameter pitot-type probe capable of resolving three components of velocity. The probe is comprised of a conical tip in which five holes are drilled; these

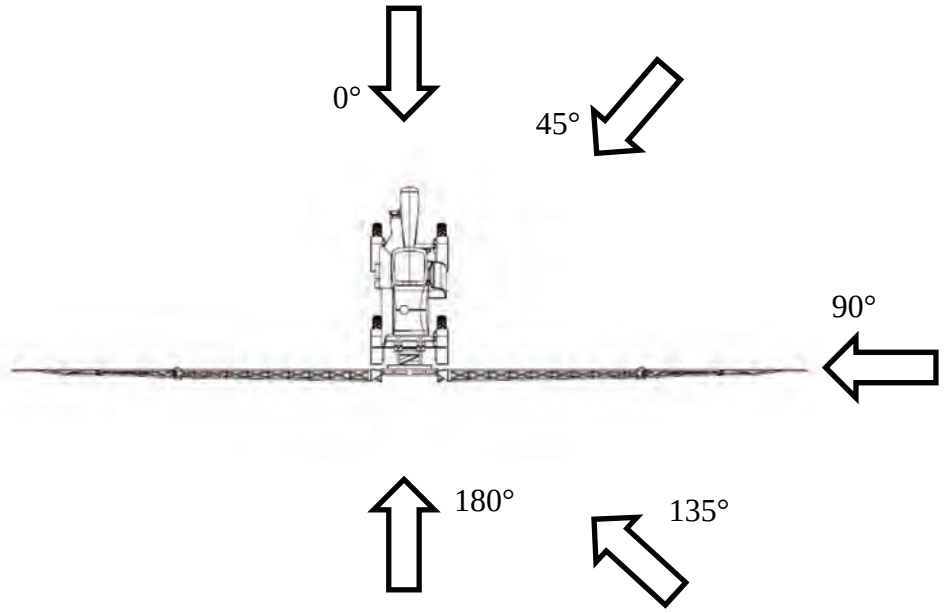

Figure 2. Wind direction vectors at 0°, 45°, 90°, 135°, and 180°. Zero is relative to the center of the spray boom. The relative *x* axis is pointed in the direction of the arrow, with the relative *y* axis pointing to the left of the *x* direction, for each of the wind directions.

Table 1. Full-scale measurement distances along the relative *x* axes for each of the five wind directions.

X (m) at 0°	*x* (m) at 45°	*x* (m) at 90°	*x* (m) at 135°	*x* (m) at 180°
-0.875	-6.375	-9.125	-6.375	-0.875
0.875	-1.875	0.0	-1.25	0.875
5.0	1.25	9.125	1.875	5.0
11.875	6.375	18.625	6.375	8.75
	13.375	28.125	13.375	11.875
	18.875		18.875	

holes lead to tubes that run through the body of the probe and are connected via flexible tubing to precision pressure transducers. A calibration file and data reduction routine convert the five measured pressures into a three-dimensional velocity vector. In this application, the probe was mounted on a computer-controlled three-axis traverse, which allowed it to be positioned anywhere around the model.

Data were acquired at a sampling rate of 1 kHz for 65.536 s per measurement point, comprising eight contiguous measurement blocks of 8192 samples each. This time interval reflected the time needed to achieve acceptably settled values of mean velocity and turbulence intensity (TI). With slightly more than 1 min of sampling, the mean velocity values settled to a standard error on average of less than 1.5% of their value, the standard deviation of the standard error percentage being less than 0.5%. Maximum standard error was always less than 4.0% of the measured value.

An initial survey of the wake was made with smoke flow visualization prior to taking data around and behind the subscale model. Based on these results, and preliminary measurements, the location and extent of the planes to be traversed were chosen. These data were then entered into the traverse control software, which automatically moved the probe to the desired locations and took measurements for the prescribed time interval. Measurements were generally made in lateral steps (for a relative *x* value) and different heights to capture the wake effect generated by the subscale model. Some of the particulars of the tests were the following:

- All tunnel measurements were done at subscale and are reported here at full scale.
- In Teske et al. (2015), the reference wind speed (U_{ref}) was 10.8 m s^{-1} measured at a height (Z_{ref}) of 1.265 m subscale by a pitotstatic tube positioned just upstream of the model. In the present work, U_{ref} was 11.1 m s^{-1} measured at Z_{ref} of 1.060 m subscale.
- Wind speed data were taken with and without the presence of the model. Missing data away from the model were assumed at their background values for velocity and turbulence level, which were collected when the model was not present in the wind tunnel. Trial runs were performed to ensure Reynolds number independence. If tests were run at too low a Reynolds number, it was possible for the flow to become laminar instead of turbulent. By taking measurements over a range of wind speeds, it was possible to determine a speed at which the nature of the flow did not change with speed.
- The model was stationary in the wind tunnel, eliminating any possibility of boom motion (such as the up-and-down effect of a moving sprayer). The boom articulation linkages were ±42 and ±58 cm subscale (±10.5 and ±14.5 m full scale) from the centerline of the tractor. Boom height was maintained by six vertical pins (three on each side of the boom) of 26 mm length (0.65 m full scale) and 2.4 mm diameter, positioned at distances of ±9, ±42, and ±69 cm subscale (±2.25, ±10.5, and ±22.5 m full scale) from the center of the tractor, as seen in the bottom photo in figure 1.

The pins did not appear to affect the wake.

- The subscale boom length was 1.45 m. Thus, the full-scale boom length would be 36.25 m, representative of large, low boom sprayers (lengths between 25 and 45 m) operating in the U.S.
- The absolute coordinate system was (*X*, *Y*, *Z*), with *X* and *Y* centered on the center of the spray boom and *Z* measured vertically from the floor of the tunnel. *X* was pointed in the downwind direction, parallel to the tunnel walls (with velocity *U*), *Y* was pointed perpendicular to the left of the *X* direction (with velocity *V*), and *Z* was pointed vertically toward the tunnel ceiling (with velocity *W*). Defined in this way, the coordinate system is identical to the system assumed in AGDISP, thus simplifying model building and comparison.
- Tunnel measurements were recorded in Excel spreadsheets for the three velocity components and the three turbulence intensities. Wind speeds are normalized by the reference wind speed (U_{ref}), while the turbulence intensities are given in percentages based on the local *U* velocity. The data included the three coordinates of the data collection points in the relative coordinates (*x*, *y*, *z*), the three velocity components (normalized by U_{ref}) in u/U_{ref}, v/U_{ref}, and w/U_{ref}, and the three turbulence intensities (normalized by the local value of $\overline{U}$ and presented in percentages) as a function of wind direction (azimuth).
- All measurements were made with the sprayer boom height at 26 mm subscale (0.65 m full scale).

TURBULENCE INTENSITY

Turbulence intensity is defined as the ratio of the standard deviation of the velocity to a mean value (Lyles et al., 1971) and is defined by the following ratios:

$$I_X = \frac{\left(\overline{u'u'}\right)^{1/2}}{\overline{U}},\ I_Y = \frac{\left(\overline{v'v'}\right)^{1/2}}{\overline{U}},\ I_Z = \frac{\left(\overline{w'w'}\right)^{1/2}}{\overline{U}} \quad (1)$$

where $\left(\overline{u'u'}\right)^{1/2}$, $\left(\overline{v'v'}\right)^{1/2}$, and $\left(\overline{w'w'}\right)^{1/2}$ are the root mean square of the fluctuating velocity components in the *X*, *Y*, and *Z* directions, respectively, and $\overline{U}$ is a mean velocity. In AGDISP (Teske et al., 2003), twice the turbulence kinetic energy is defined as q^2, such that:

$$q^2 = \overline{u'u'} + \overline{v'v'} + \overline{w'w'} \quad (2)$$

Thus, the turbulence intensity data provided from the tests can be interpreted as:

$$\frac{q^2}{U_{ref}^2} = \left(I_X{}^2 + I_Y{}^2 + I_Z{}^2\right)\left(\frac{\overline{U}}{U_{ref}}\right)^2 \quad (3)$$

RESULTS

The first step in data reduction was to examine the data taken without the model present in the wind tunnel (identified as "tunnel background" in the datasets). Six thousand velocity measurements were made in an effort to determine representative background velocities and turbulence for the five wind directions. As shown previously by Teske et al. (2015), the behavior of the (small) background vertical velocity (*w*) is ascribed to the structure of the roughness elements around and behind the model, while the left-to-right crosswind velocity (*v*) is small. Fitting the data to logarithmic profiles, such that $\overline{U}/U_{ref} = 1$ at $Z = Z_{ref}$ gives:

$$\frac{\overline{U}}{U_{ref}} = \frac{U_0}{U_{ref}} \ln\left(\frac{Z}{z_0}\right) \quad (4)$$

where U_0/U_{ref} and z_0 are summarized in table 2 (weighted average $R^2 = 0.612$). These results vary with wind direction because the roughness elements near the model are different for each wind direction.

Table 2. Logarithmic curve fit parameters (full scale). The computed z_0 values are suggestive of 10 to 18 cm high grass (Hansen, 1993).

Wind Direction	z_0 (m)	U_0/U_{ref}
0° for *X* = -0.875 m	0.0184	0.138
0° for *X* = 0.875, 5.0, and 11.875 m	0.0443	0.152
45° for all *X*	0.0130	0.128
90° for all *X*	0.0071	0.119
135° for all *X*	0.0275	0.146
180° for all *X*	0.0345	0.151

The six logarithmic profiles for u/U_{ref} (for all wind directions) are averaged and plotted in figure 3, along with the average velocity ratios from the six sets of tunnel data shown

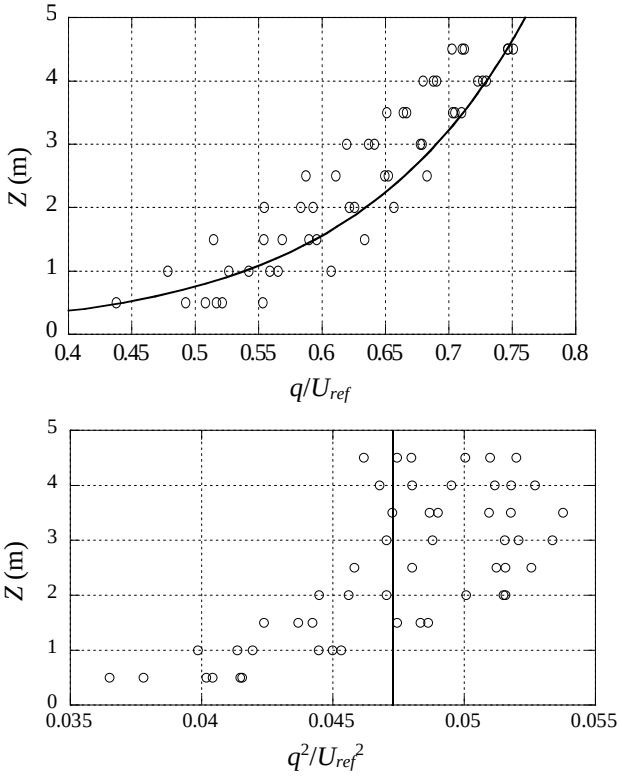

Figure 3. (top) Behavior of the averages of the six sets of data (table 2) for u/U_{ref} compared with the logarithmic curve fits, and (bottom) behavior of corresponding averaged turbulence levels, including the overall average value of 0.0466, based on the logarithmic profiles determined from the six sets of data (eq. 5 and table 2).

Table 3. Average vertical and crosswind velocities.

Wind Direction	v/U_{ref}	w/U_{ref}
0°	0.00512	-0.03070
45°	0.00693	0.03089
90°	-0.00114	-0.01180
135°	0.00099	-0.01686
180°	0.00332	-0.02098

in table 2. The weighted average background values for v/U_{ref} and w/U_{ref} are 0.00308 and -0.00457, respectively (specific wind directions and their variability are shown in table 3). Figure 3 also plots the six sets of turbulence data (for all wind directions) computed with the approach summarized above. The average turbulence level is included in this figure. The turbulence level can be related to the logarithmic velocity profile, through the invariant second-order closure turbulence model developed by Donaldson (1973) and discussed by Lewellen (1977), by the expression:

$$\frac{q^2}{U_{ref}{}^2} = 2\Lambda^2\left(\frac{d}{dz}\left[\frac{\overline{U}}{U_{ref}}\right]\right)^2 = 2\alpha^2\left(\frac{U_0}{U_{ref}}\right)^2 \qquad (5)$$

from equation 4, where $\Lambda = \alpha z$ is the assumed form for the turbulent macroscale near the surface. The test results give a weighted average of $\alpha = 0.91$, assuming that the turbulent kinetic energy is partitioned as $\overline{u'u'}/q^2 = 0.5$ and $\overline{v'v'}/q^2 = \overline{w'w'}/q^2 = 0.25$. The value of α is typically between 0.40 (von Kármán constant) and 1.0 (physical upper limit), as discussed by Launder et al. (1975) and Umlauf and Burchard (2005).

Collected flow results with the model in place are shown in figures 4 to 8 for v and w and in figures 9 to 13 for u and q^2. As may be seen in these figures:

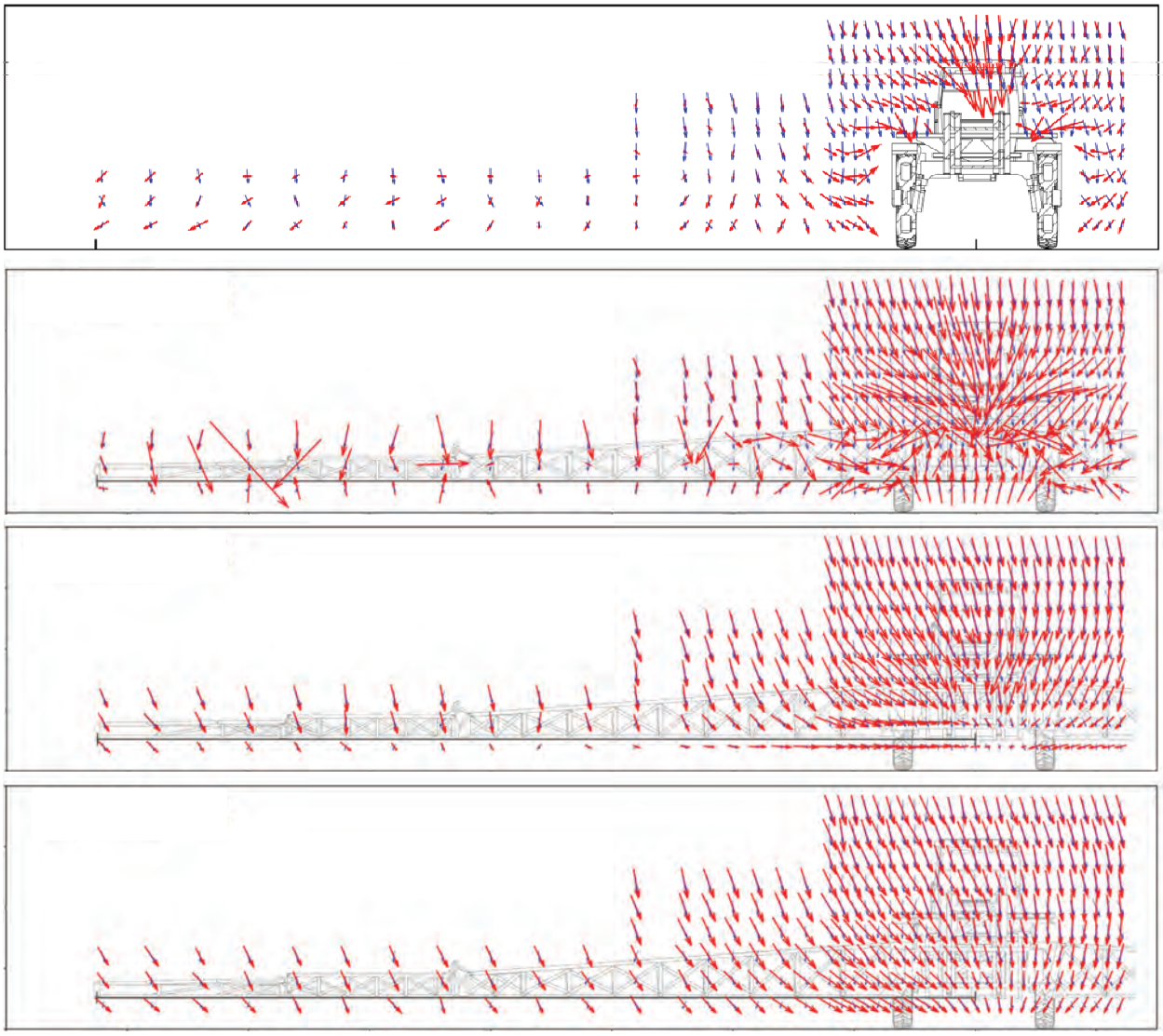

Figure 4. A wind direction of 0° (head wind) results in the directions and relative magnitudes of the V/U_{ref} (horizontal) and W/U_{ref} (vertical) velocities shown around the spray rig (red arrows). Blue arrows show the nearly vertical velocity pattern with the subscale model not present in the wind tunnel. The top plot shows the flow measured at a distance of 0.875 m upwind of the spray boom. The plots below the top plot show the flow measured at distances of 0.875, 5.0, and 11.875 m downwind of the spray boom, respectively. The apparent boom anomalies 0.875 m downwind are the result of the boom articulation points. The length of the longest arrow at the outer articulation point, at a distance of 0.875 m downwind, represents a speed of 0.2378 U_{ref}.

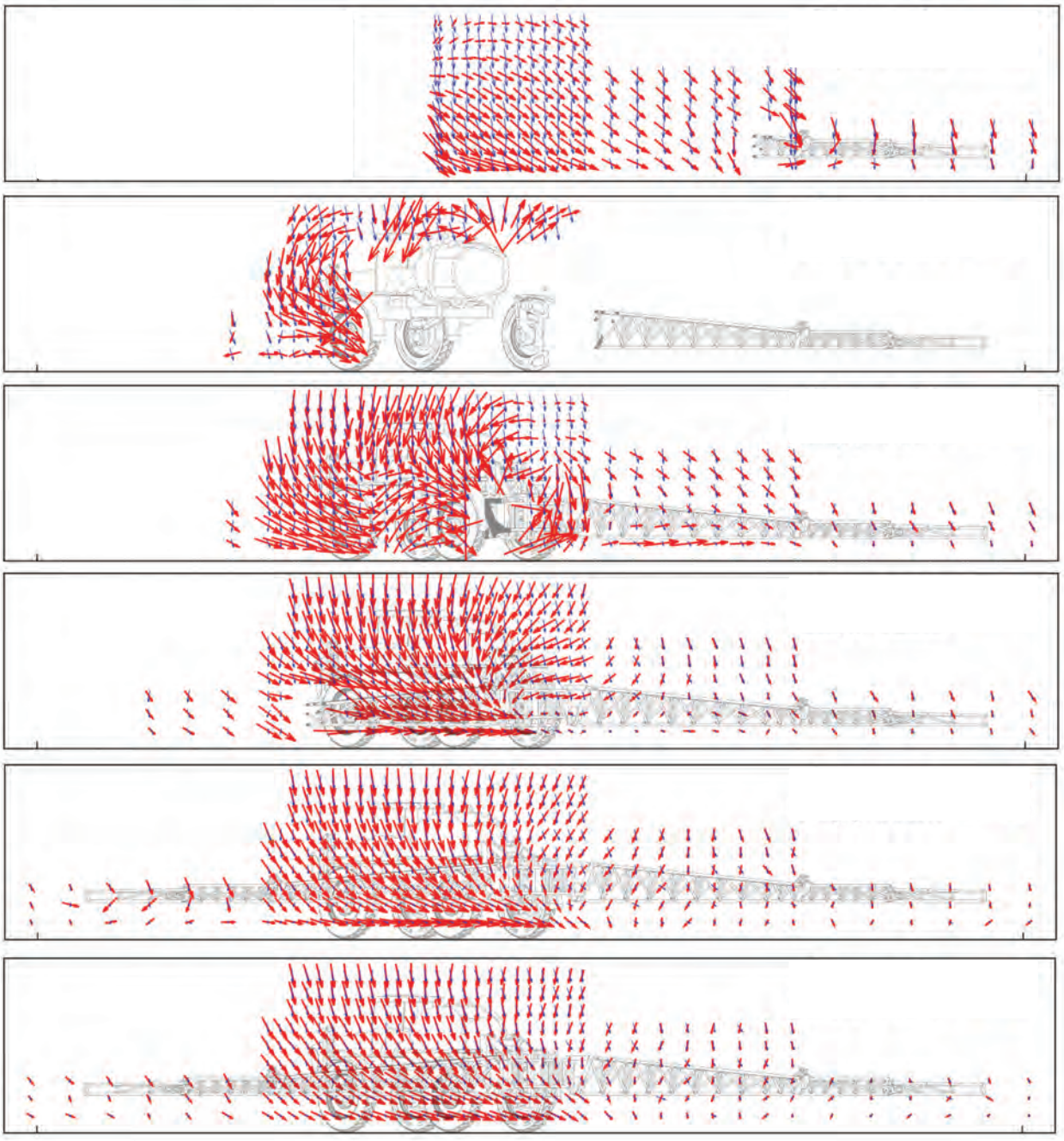

Figure 5. A wind direction of 45° results in the directions and relative magnitudes of the v/U_{ref} (horizontal) and w/U_{ref} (vertical) velocities shown around the spray rig (red arrows). Blue arrows show the nearly vertical velocity pattern with the subscale model not present in the tunnel. The top plot shows the flow measured at a distance of 6.375 m upwind of the spray boom centerline. The plots below the top plot show the flow measured at a distance of 1.875 m upwind and distances of 1.25, 6.375, 13.375, and 18.875 m downwind of the spray boom centerline, respectively. The length of the longest arrows over the top of the tractor, at a distance of 1.875 m upwind, represents a speed of 0.2132 U_{ref}.

- The presence of the model stirs the velocity field. These figures demonstrate the variation from background conditions that could be expected for the velocity profiles in the wake of a spray rig and suggest the potential downwind influence of the tractor/tank/spray boom combination.
- In figures 4 and 9 (0°), the tractor blocks the flow (0.875 m upwind of the tractor/boom), which then fills in behind the tractor (0.875 m downwind) and slowly returns to background values farther downwind. The upwash immediately behind the wheels is caused by accelerated flow from under the tractor body.
- In figures 5 and 10 (45°), the cross flow is deflected toward the front of the spray boom and then quickly becomes vertical behind the boom (6.375 m upwind). Flow around the top of the tractor body is first seen at 1.875 m upwind and moves around the tractor toward the spray boom as the measurement plane advances downwind.
- In figures 6 and 11 (90°), the cross flow moves over the top and front of the tractor (0.0 m) and then rushes to fill the void behind the tractor.

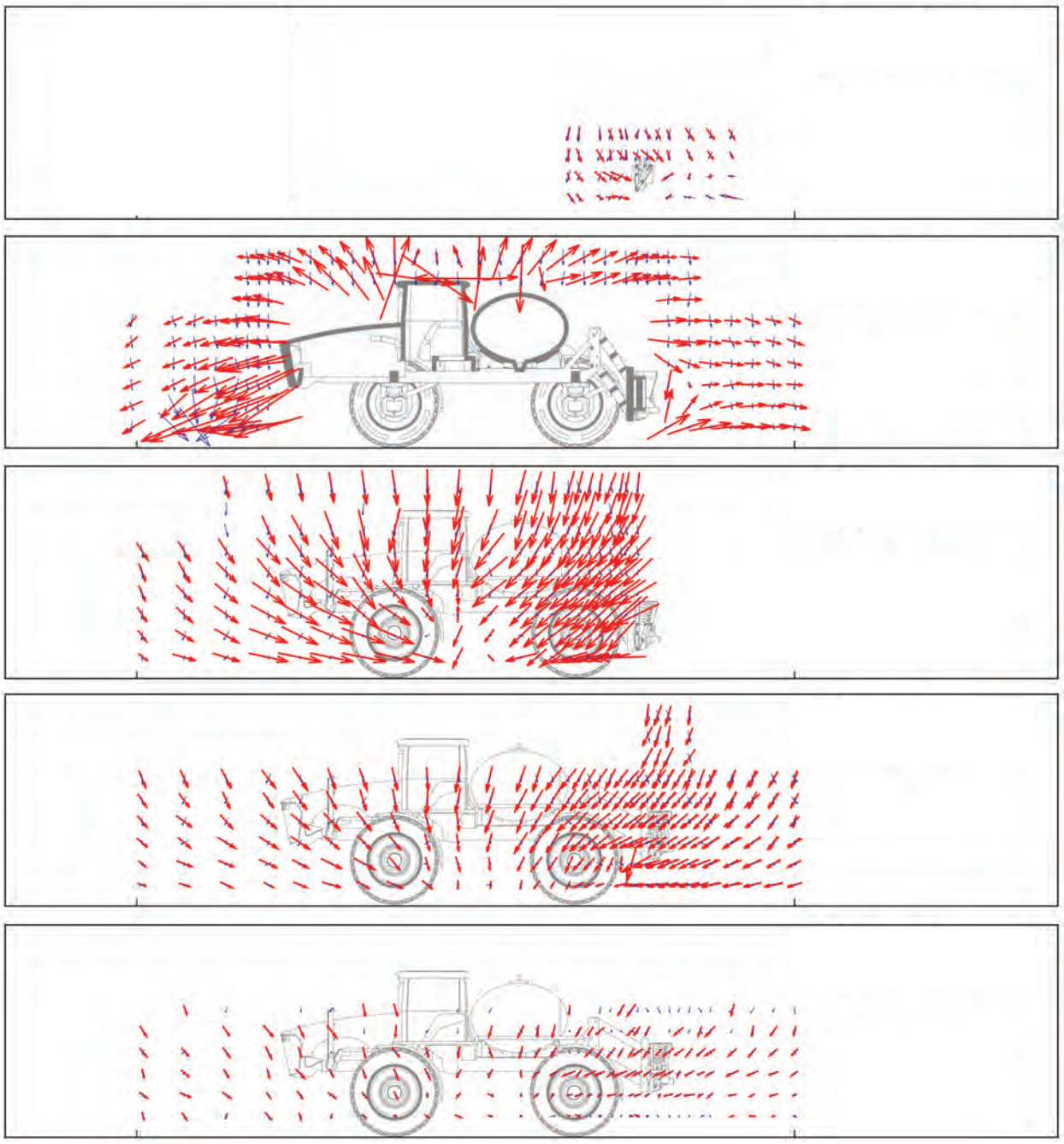

Figure 6. A wind direction of 90° (side wind) results in the directions and relative magnitudes of the v/U_{ref} (horizontal) and w/U_{ref} (vertical) velocities around the spray rig (red arrows). Blue arrows show the nearly vertical velocity pattern with the subscale model not present in the tunnel. The top plot shows the flow measured at a distance of 9.125 m upwind of the spray boom centerline. The plots below the top plot show the flow measured at the centerline (0.0 m) and at distances of 9.125, 18.625, and 28.125 m downwind of the spray boom centerline, respectively. The length of the longest arrows over the top of the tractor, at a distance of 0.0 m, represents a speed of 0.2086 U_{ref}.

- In figures 7 and 12 (135°), the flow around the tires is more apparent (especially at 6.375 m downwind), followed by flow filling in the tractor wake.
- In figures 8 and 13 (180°), the behavior of the flow around and downwind of the tractor body is well defined by the test data.

DISCUSSION

The velocity profiles illustrated in figures 4 to 8, along with their corresponding u/U_{ref}, v/U_{ref}, w/U_{ref}, and q^2/U_{ref}^2 profiles, were recorded at discrete vertical increments of 0.5 m (full scale) for five wind directions. Inserting this information into a computer code is accomplished by interpolating the data linearly between heights. The only height where this approach presents a problem is between the floor of the tunnel and 0.5 m, where the following are assumed: a logarithmic profile for u/U_{ref} (given in eq. 4), a linear profile for v/U_{ref} and w/U_{ref} between a surface value of 0.0 and their measured values at 0.5 m, and a constant value for q^2/U_{ref}^2 (given in eq. 5) from its measured value at 0.5 m. Wind di-

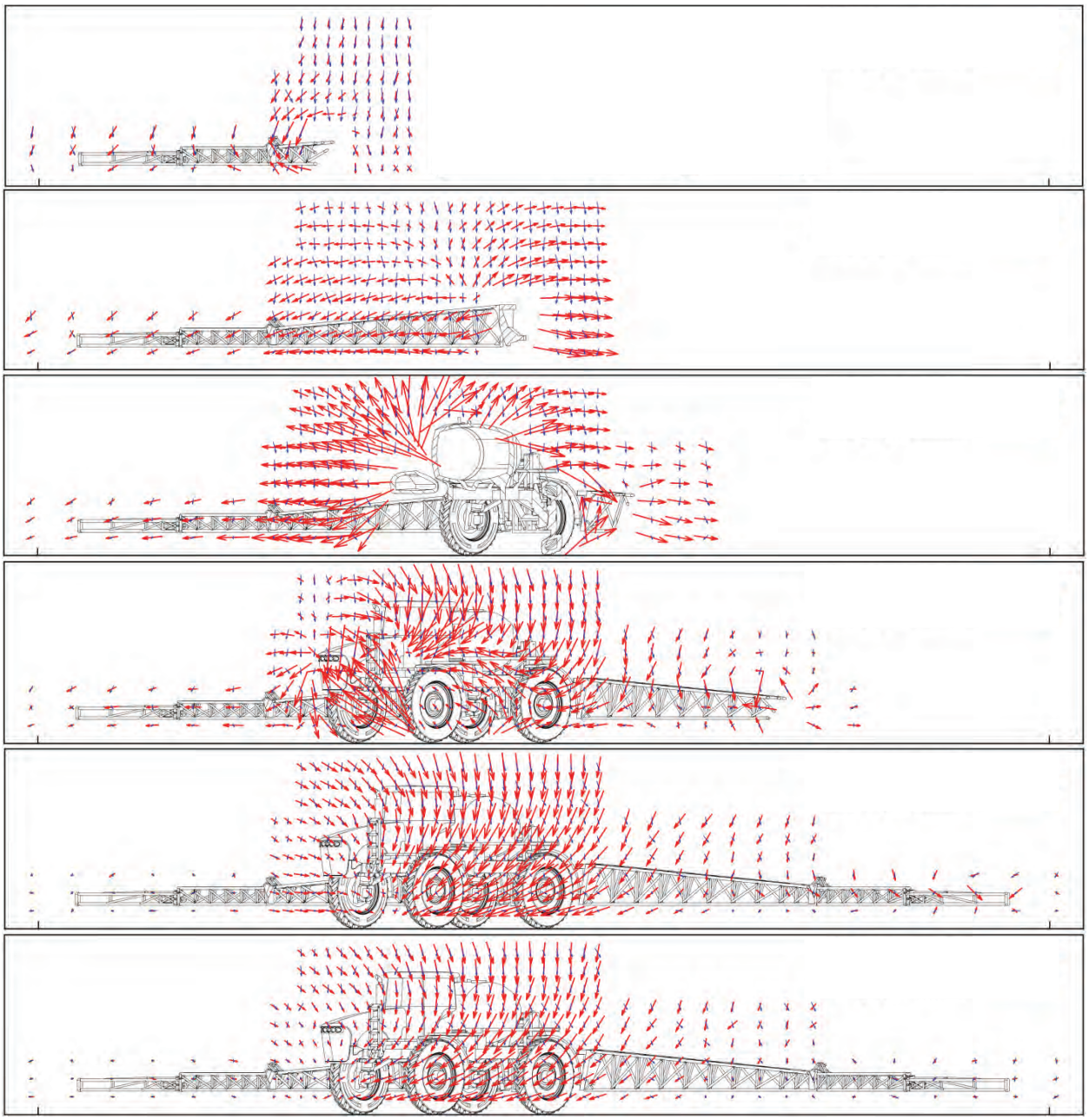

Figure 7. A wind direction of 135° results in the directions and relative magnitudes of the v/U_{ref} (horizontal) and w/U_{ref} (vertical) velocities shown around the spray rig (red curves). Blue arrows show the nearly vertical velocity pattern with the subscale model not present in the tunnel. The top plot shows the flow measured at a distance of 6.375 m upwind of the spray boom centerline. The plots below the top plot show the flow measured at a distance of 1.25 m upwind and at distances 1.875, 6.375, 13.375, and 18.875 m downwind of the spray boom centerline, respectively. The length of the longest arrows, around the underside of the tractor at a distance of 6.375 m, represents a speed of 0.2256 U_{ref}.

rection is interpolated by first transforming the desired (X, Y, Z) point into the (x, y, z) point:

$$\begin{aligned} x &= X\cos\theta - Y\sin\theta \\ y &= X\sin\theta + Y\cos\theta \end{aligned} \tag{6}$$

where θ is the wind direction measured from 0°. The interpolated data from the two bounding wind directions are combined trigonometrically (0° to 45°, 45° to 90°, 90° to 135°, or 135° to 180°) to give u/U_{ref}, v/U_{ref}, w/U_{ref}, and q^2/U_{ref}^2 and then inverse transformed:

$$\begin{aligned} \frac{U}{U_{ref}} &= \frac{u}{U_{ref}}\cos\theta + \frac{v}{U_{ref}}\sin\theta \\ \frac{V}{U_{ref}} &= -\frac{u}{U_{ref}}\sin\theta + \frac{v}{U_{ref}}\cos\theta \end{aligned} \tag{7}$$

Model predictions can then be obtained for any wind direction and any location around the spray rig, since the flow field is symmetrical about 0° and 180°. These additional subroutines were inserted into a simple adaptation of AGDISP used previously to compute spray deposition from a portion of a full-scale spray boom (Teske et al., 2016). Model results

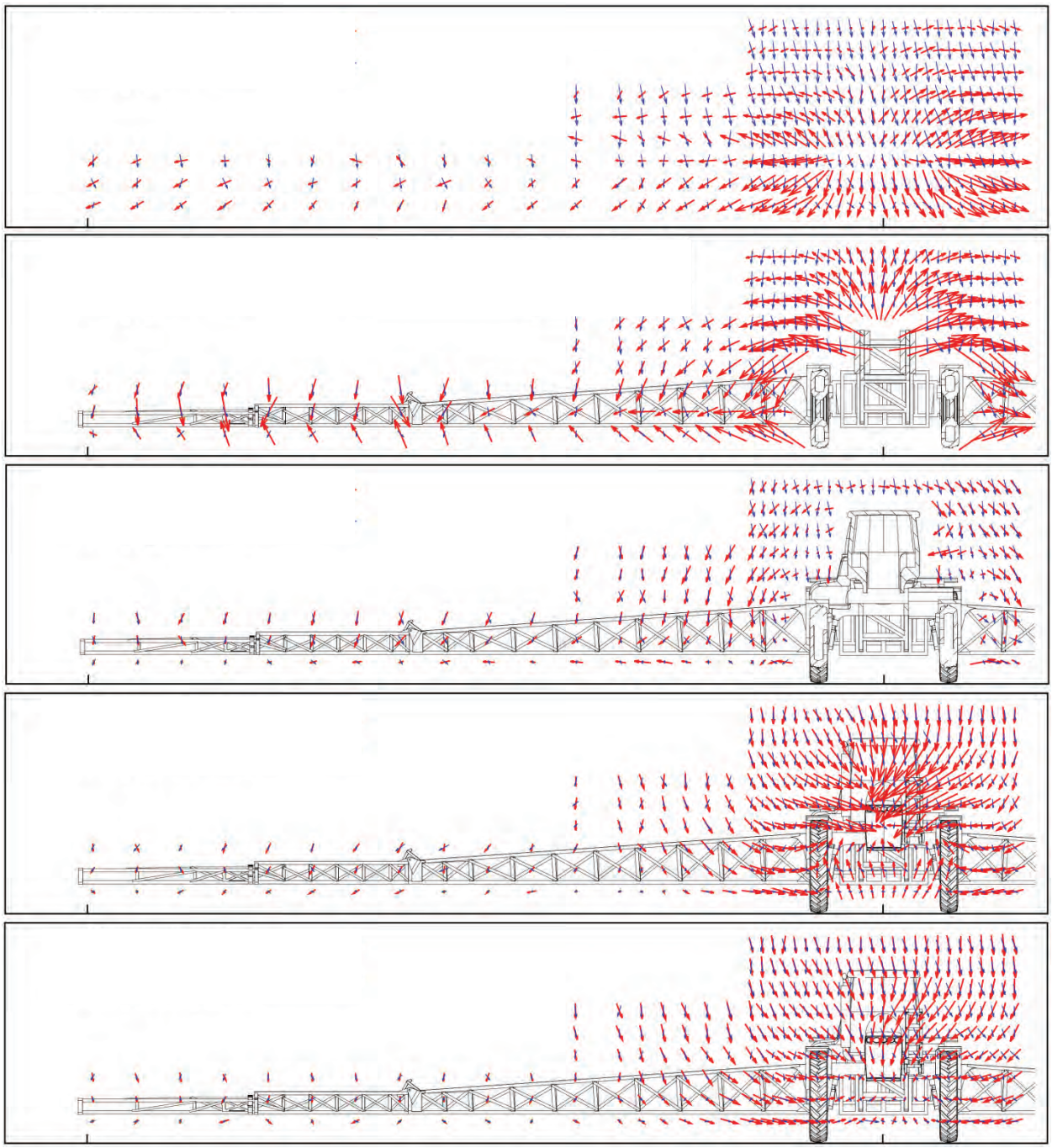

Figure 8. A wind direction of 180° (tail wind) results in the directions and relative magnitudes of the w/U_{ref} (horizontal) and w/U_{ref} (vertical) velocities shown around the spray rig (red curves). Blue arrows show the nearly vertical velocity pattern with the subscale model not present in the wind tunnel. The top plot shows the flow measured at a distance of 0.875 m upwind of the spray boom. The plots below the top plot show the flow measured at distances 0.875, 5.0, 8.75, and 11.875 m downwind of the spray boom, respectively. The length of the largest arrow, along the backside of the tractor at a distance of 0.875 m, represents a speed of 0.1428 U_{ref}.

(driven by a random number generator for meteorological inputs) are compared in figures 14 and 15 for a tractor speed of 6 m s^{-1}, wind speed of 5 m s^{-1} ±1 m s^{-1}, temperature of 22.5°C ±2.5°C, and relative humidity of 65% ±5%.

Figure 14 illustrates the wind direction variation, while figure 15 illustrates the change in droplet size distribution. Waviness in the downwind deposition patterns is the result of droplets hitting the surface at irregular intervals. Of interest in figure 14 is that the wind direction of -135° (hitting near the back of the tractor) appears somewhat smoother than the wind direction of -45° (hitting near the front of the tractor), whereas the tail wind causes a slightly wider deposition pattern than the headwind. Likewise in figure 15, as the droplet size distribution increases in coarseness, the deposition pattern reflects less drift downwind.

Conclusions and Recommendations

This article examines wind tunnel test data generated over a subscale (1:25) spray rig model. The generic model permits

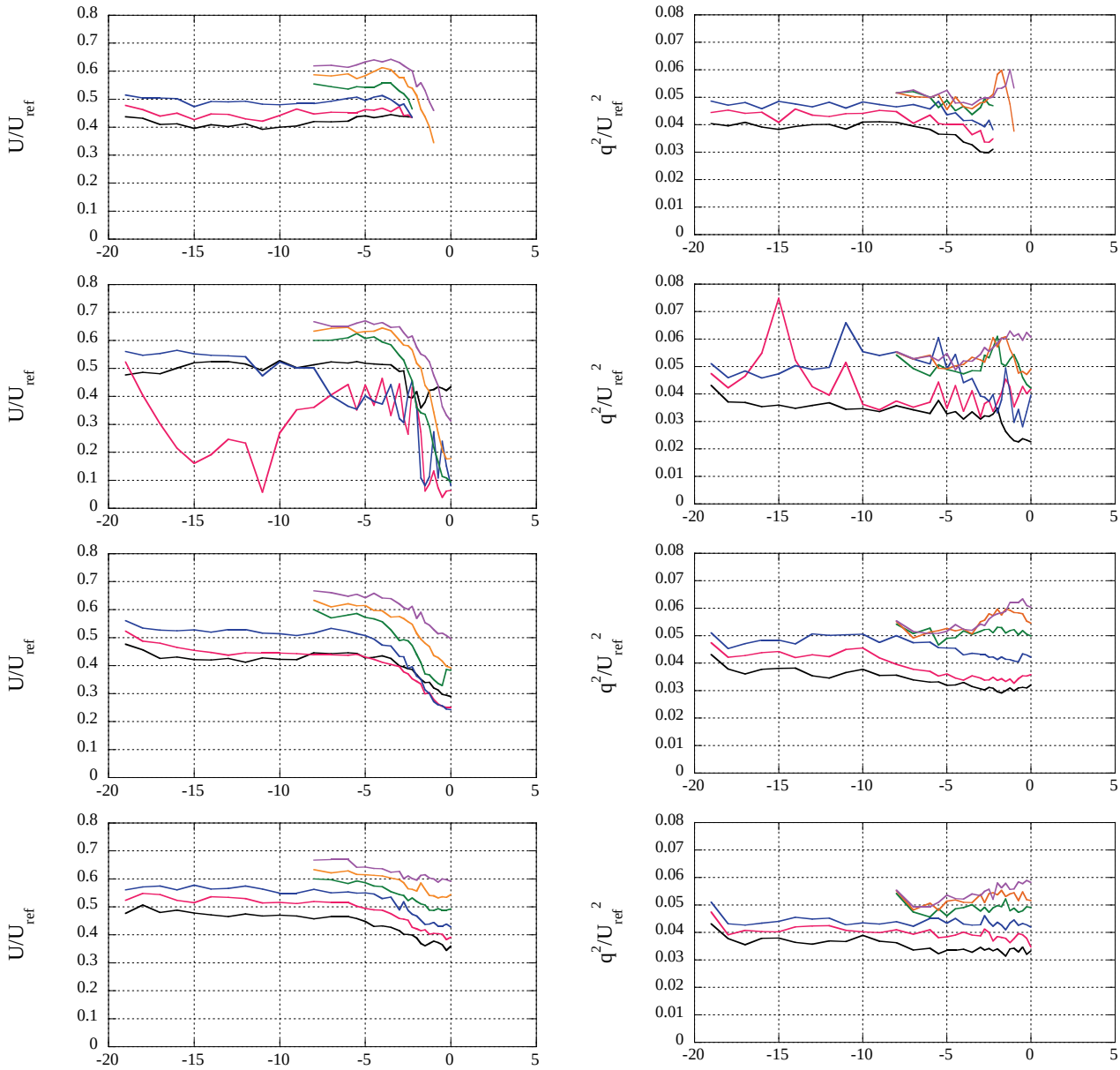

Figure 9. Velocity (U/U_{ref}) and turbulence (q^2/U_{ref}^2) values for a wind direction of 0° (head wind). The top plot describes the flow measured at a distance of 0.875 m upwind of the spray boom. The plots below the top plot describe the flow measured at distances of 0.875, 5.0, and 11.875 m downwind of the spray boom, respectively. The traces are for heights Z = 0.5 m (black curves), 1 m (red curves), 1.5 m (blue curves), 2 m (green curves), 2.5 m (orange curves), and 3 m (purple curves) as a function of horizontal distance Y in m. The tractor centerline is at Y = 0 m. The apparent anomalies 0.875 m downwind are the result of the boom articulation points.

the measurement of wind speeds and turbulence fluctuations near the model, recovering the local wind field that provides the ambient background into which spray material may be released from the boom. As such, these subscale tests can be used to represent tractor/tank/spray boom wake features that have to this point been neglected in existing ground sprayer models. The wind tunnel tests demonstrate the usefulness and practicality of data collected in this manner.

The computer code developed under this effort will serve as the starting point for further work in this area, including computational fluid dynamics (CFD) modeling of the sub-scale model.

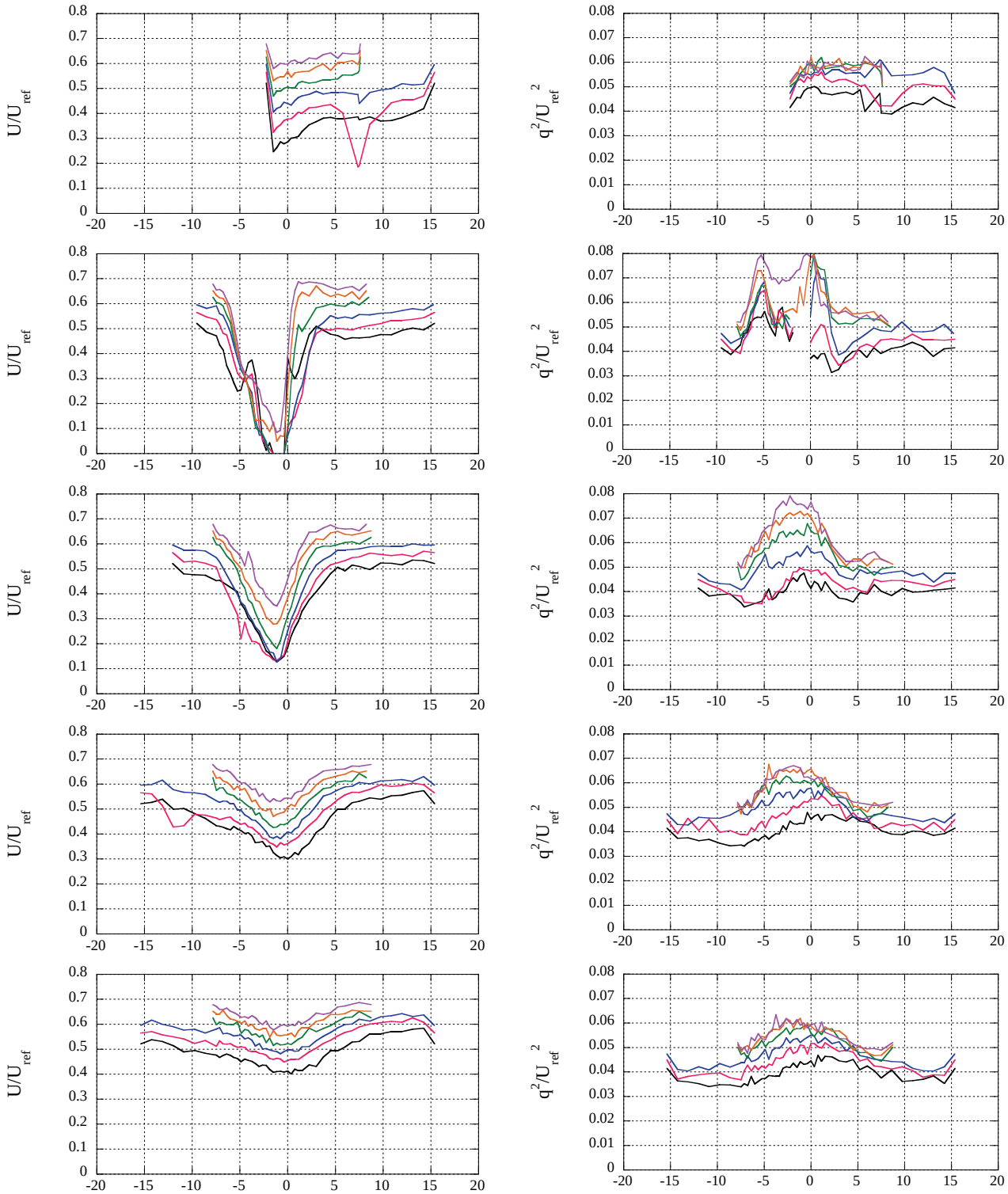

Figure 10. Velocity (u/U_{ref}) and turbulence (q^2/U_{ref}^2) values for a wind direction of 45°. The top plot describes the flow measured at a distance of 6.375 m upwind of the sprayer centerline. The plots below the top plot describe the flow measured at distances of 1.25, 6.375, 13.375, and 18.875 m downwind of the sprayer centerline, respectively. The traces are for heights Z = 0.5 m (black curves), 1 m (red curves), 1.5 m (blue curves), 2 m (green curves), 2.5 m (orange curves), and 3 m (purple curves) as a function of horizontal distance y in m. The effect of the tractor body is most evident 1.25 and 6.375 m downwind.

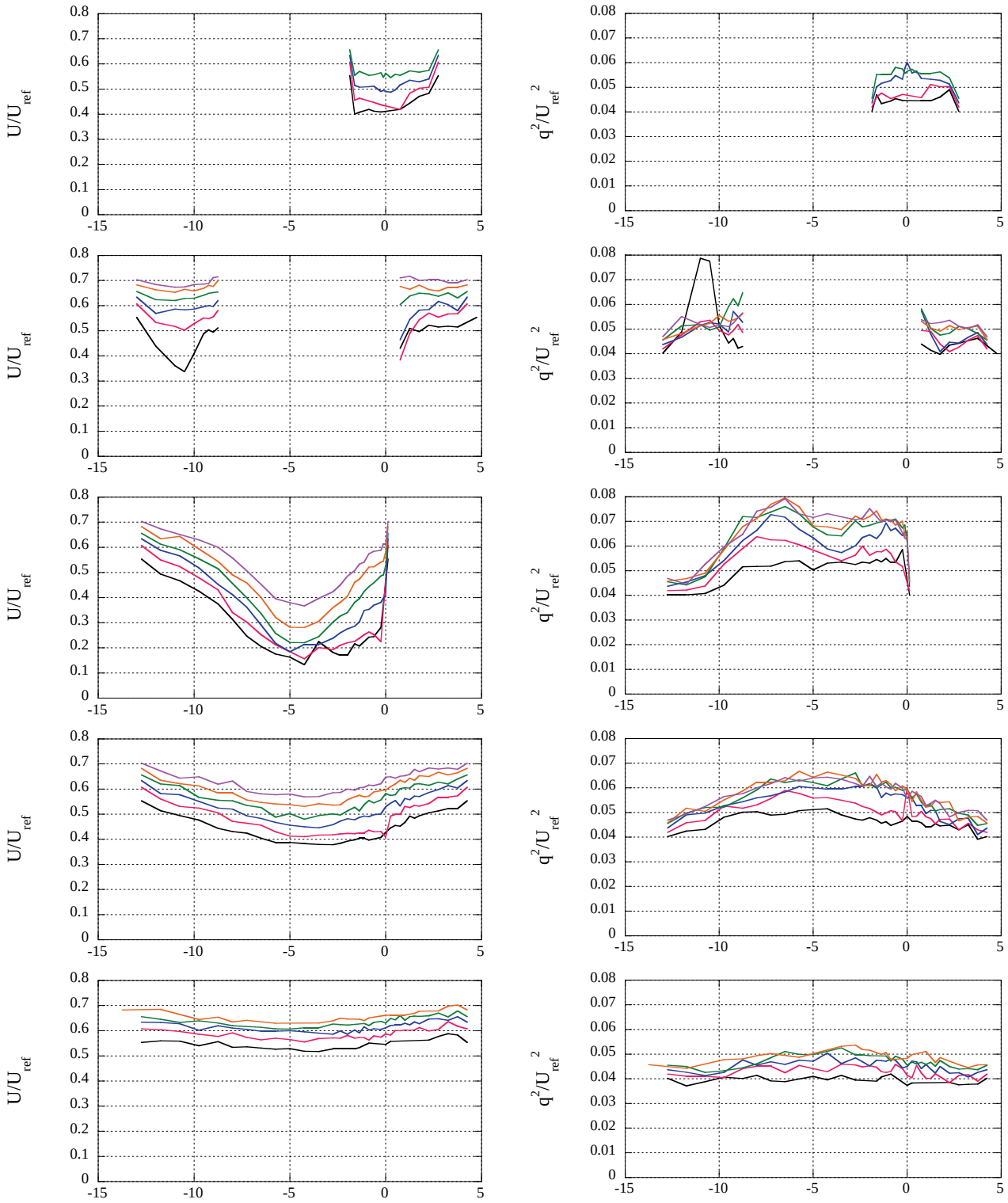

Figure 11. Velocity (u/U_{ref}) and turbulence (q^2/U_{ref}^2) values for a wind direction of 90° (side wind). The top plot describes the flow measured at a distance of 9.125 m upwind of the spray boom centerline. The plots below the top plot describe the flow measured at distances of 0.0, 9.125, 18.625, and 28.125 m downwind of the spray boom centerline, respectively. The traces are for heights Z = 0.5 m (black curves), 1 m (red curves), 1.5 m (blue curves), 2 m (green curves), 2.5 m (orange curves), and 3 m (purple curves) as a function of horizontal distance y in m. The tractor body cuts off data collection at 0.0 m downwind.

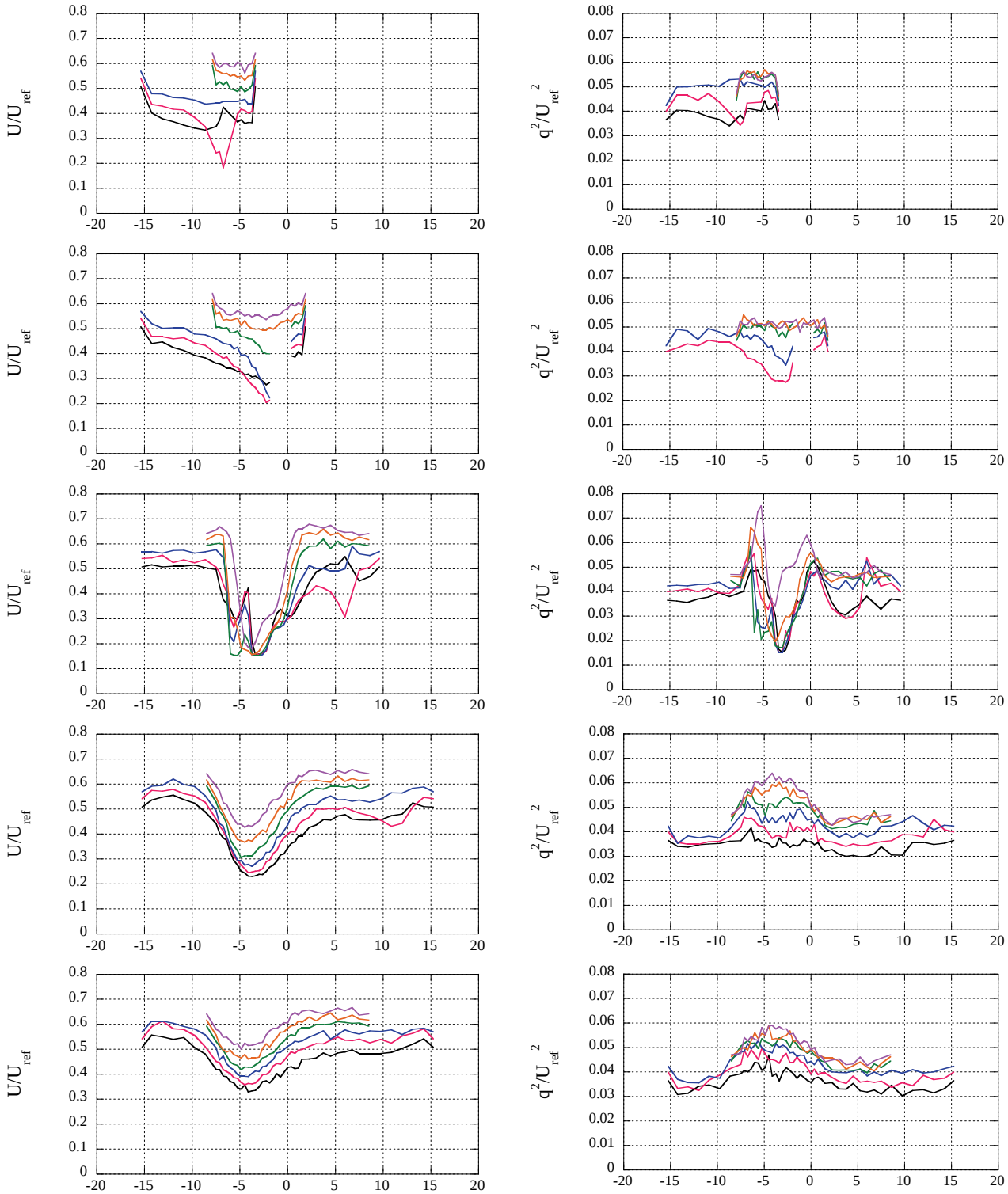

Figure 12. Velocity (u/U_{ref}) and turbulence (q^2/U_{ref}^2) values for a wind direction of 135°. The top plot describes the flow measured at a distance of 6.375 m upwind of the sprayer centerline. The plots below the top plot describe the flow measured at a distance of 1.25 m upwind and at distances of 6.375, 13.375, and 18.875 m downwind of the sprayer centerline, respectively. The traces are for heights Z = 0.5 m (black curves), 1 m (red curves), 1.5 m (blue curves), 2 m (green curves), 2.5 m (orange curves), and 3 m (purple curves) as a function of horizontal distance y in m. The presence of the tractor body is seen most clearly 6.375 m downwind.

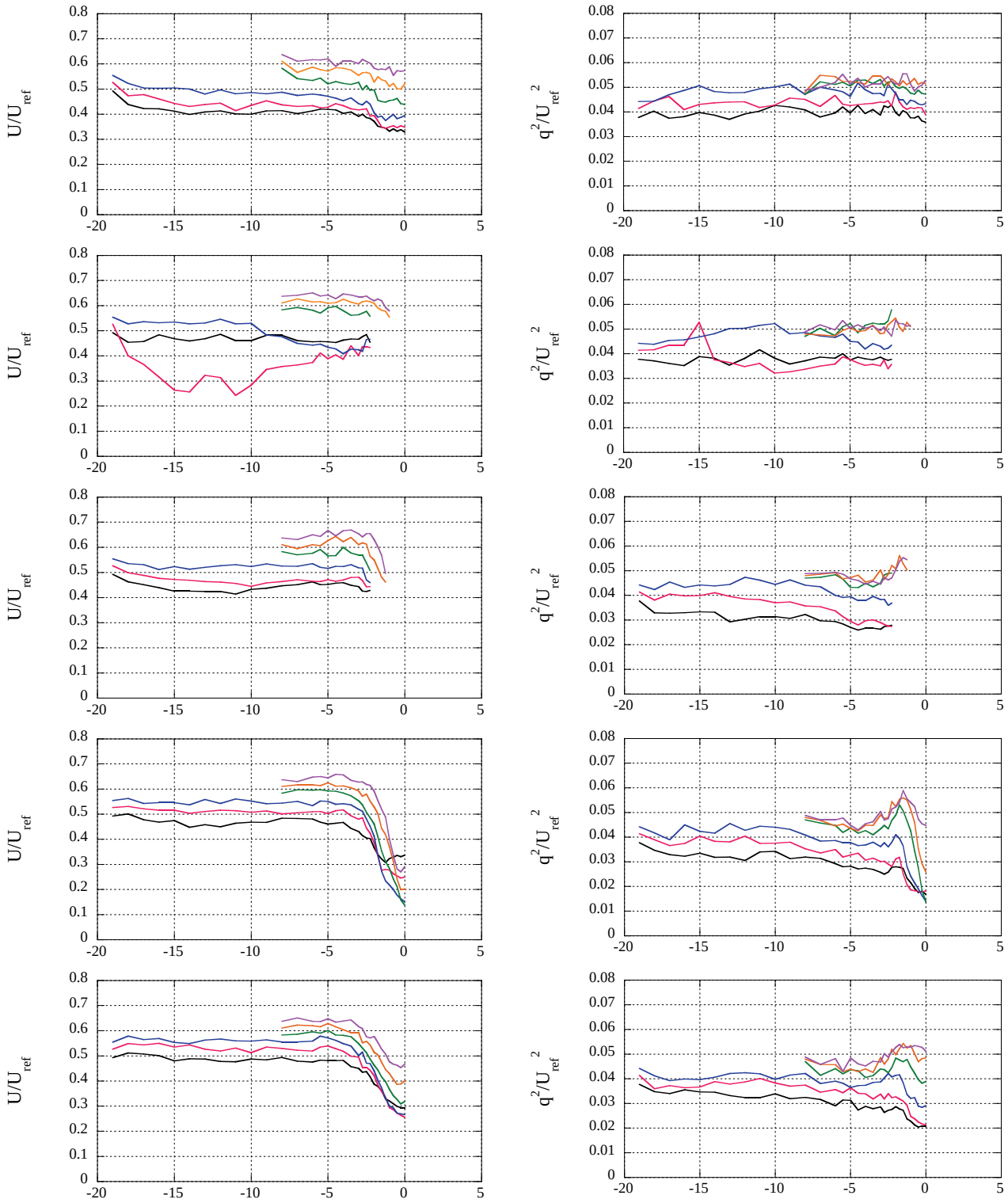

Figure 13. Velocity (u/U_{ref}) and turbulence (q^2/U_{ref}^2) values for a wind direction of 180° (tail wind). The top plot describes the flow measured at a distance of 0.875 m upwind of the spray boom. The plots below the top plot describe the flow measured at distances of 0.875, 5.0, 8.75, and 11.875 m downwind of the spray boom, respectively. The traces are for heights Z = 0.5 m (black curves), 1 m (red curves), 1.5 m (blue curves), 2 m (green curves), 2.5 m (orange curves), and 3 m (purple curves) as a function of horizontal distance y in m. The tractor centerline is at y = 0 m. The apparent boom anomaly 0.875 m downwind is the result of the boom articulation points.

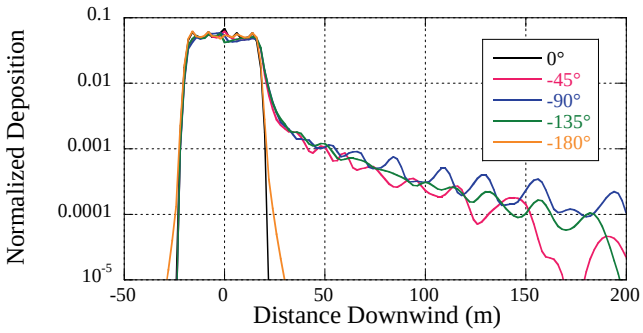

Figure 14. Model comparison illustrating the effect of wind direction for ASABE Very Fine to Fine (VFF) droplet size distribution.

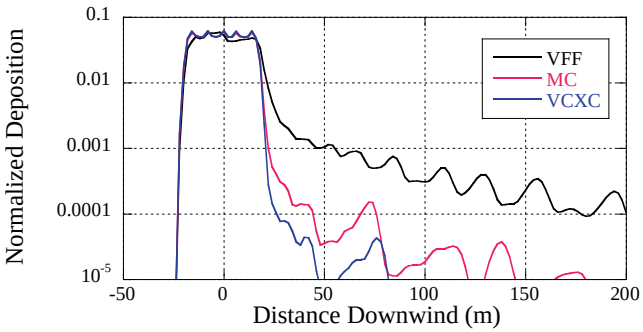

Figure 15. Model comparison illustrating the effect of droplet size distribution for a crosswind at -90°: ASABE droplet size distributions of Very Fine to Fine (VFF), Medium to Coarse (MC), and Very Coarse to Extremely Coarse (VCXC).

REFERENCES

Donaldson, C. du P. (1973). Atmospheric turbulence and the dispersal of atmospheric pollutants. In D. A. Haugen (Ed.), *AMS workshop on micrometeorology* (pp. 313-390). Boston, MA: Science Press. See also: EPA-R4-73-016a, Office of Research and Monitoring, U. S. Environmental Protection Agency, Washington, DC.

Hansen, F. V. (1993). Surface roughness lengths. Report No. ARL-TR-61. White Sands Missile Range, NM: U.S. Army Research Laboratory.

Launder, B. E., Reece, G. J., & Rodi, W. (1975). Progress in the development of a Reynolds-stress turbulence closure. *J. Fluid Mech., 68*(3), 537-566. http://dx.doi.org/10.1017/S0022112075001814

Lewellen, W. S. (1977). Use of invariant modeling. In W. Frost, & T. H. Moulden (Eds.), *Handbook of turbulence* (Vol. I, pp. 237-280). New York, NY: Plenum. http://dx.doi.org/10.1007/978-1-4684-2322-8_9

Lyles, L., Disrud, L. A., & Krauss, R. K. (1971). Turbulence intensity as influenced by surface roughness and mean velocity in a wind-tunnel boundary layer. *Trans. ASAE, 14*(2), 285-289. http://dx.doi.org/10.13031/2013.38277

Teske, M. E., Miller, P. C. H., Thistle, H. W., & Birchfield, N. B. (2009). Initial development and validation of a mechanistic spray drift model for ground boom sprayers. *Trans. ASABE, 52*(4), 1089-1097. http://dx.doi.org/10.13031/2013.27779

Teske, M. E., Thistle, H. W., & Ice, G. G. (2003). Technical advances in modeling aerially applied sprays. *Trans. ASAE, 46*(4), 985-996. http://dx.doi.org/10.13031/2013.13955

Teske, M. E., Thistle, H. W., Gross, G. M., Lawton, T. C. R., Petersen, R. L., & Funseth, T. G. (2015). Evaluation of the wake of an agricultural ground sprayer. *Trans. ASABE, 58*(3), 621-628. http://dx.doi.org/10.13031/trans.58.10996

Teske, M. E., Thistle, H. W., Lawton, T. C. R., & Petersen, R. L. (2016). Evaluation of the flow downwind of an agricultural ground sprayer boom. *Trans. ASABE, 59*(3), 839-846. http://dx.doi.org/10.13031/trans.59.11442

Umlauf, L., & Burchard, H. (2005). Second-order turbulence closure models for geophysical boundary layers: A review of recent work. *Cont. Shelf Res., 25*(7), 795-827.